Contents lists available at ScienceDirect

Nano Energy

journal homepage: http://ees.elsevier.com

Wave impact energy harvesting through water-dielectric triboelectrification with single-electrode triboelectric nanogenerators for battery-less systems

Ulises Tronco Jurado [a,b,*], Suan Hui Pu [a,c], Neil M. White [b]

[a] Mechatronics Research Group, University of Southampton, Southampton, SO17 1BJ, UK
[b] Smart Electronic Materials and Systems Research Group, University of Southampton, Southampton, SO17 1BJ, UK
[c] University of Southampton Malaysia, Iskandar Puteri, 79200, Johor, Malaysia

ARTICLE INFO

Keywords
Water-dielectric
Breaking wave impact
Triboelectrification
Liquid environments
Battery-less

ABSTRACT

This paper evaluates the effect of water-dielectric interfaces for wave impact energy harvesting at low frequencies (0.7 Hz–3 Hz) on the output performance of Water-Dielectric Single Electrode Mode Triboelectric Nanogenerators (WDSE-TENG). The triboelectric effect is generated between water (with a net positive charge) and a hydrophobic dielectric layer (with a net negative charge). Different WDSE-TENG configurations were tested using distinct hydrophobic materials. The water-fluorinated ethylene propylene (FEP) combination resulted in the best output performance. On the contrary, an output performance reduction by a factor of 3.53 was measured with seawater-dielectric interfaces. This can be compensated by increasing the contact area, with the best performance obtained using silicone rubber compound (Acetoxy, Elastomer) utilizing a WDSE-TENG with two-dielectric layer configuration. Employing seawater as a triboelectric material, the highest electrical output power and power density of 79.18 mW and 0.344 mW/cm^2 was generated with a grid of WDSE-TENG, comprising five devices connected in parallel. The output voltage, current, transferred charge, stored energy and energy conversion efficiency (ECE) values of the grid of connected WDSE-TENG devices were compared against a single device. Such energy harvesters were able to power an ultrasonic range sensor and a one-way wireless transmitter for motion detection, distance measurement, and monitoring weather conditions. The stored energy and generated power were ~5.96 mJ and ~5.18 mW, respectively. Furthermore, the integration of the grid of WDSE-TENG with a power management control circuit (PMCC) is able to increase the output power and hence offer the potential to power up electronic devices with power consumption requirements between 1 mW and 100 mW. The results demonstrate that the grid of WDSE-TENG offers an innovative energy harvesting approach using water as a triboelectric material. The device can be used as an energy source for smart battery-less wireless sensing systems at water-structure interfaces in aquaculture (e.g. for fish detection or water level measurement) and weather condition monitoring.

1. Introduction

The harvesting of renewable hydropower sources, generated from water motion, has attracted great interest for many years [1,2]. In particular, previous work has focused on collecting the energy generated by the random motion of shallow ocean waves at low frequencies ranging from 0.5 Hz to 10 Hz, using hybrid devices combined with triboelectric nanogenerators (TENG)-electromagnetic generators (EMG) [3,4], and different TENG with solid-solid material interfaces in contact under dry conditions [5–11], and water-solid interfaces [12–21]. Besides, harvesting breaking wave impact energy [22] have been reported previously through the use of dielectric-metal contact-separation mode triboelectric nanogenerators (DMCS-TENG) [23–25] with solid materials in contact over a wide frequency range between 0.7 Hz and 252 Hz. Water-dielectric single electrode mode triboelectric nanogenerator (WDSE-TENG) operating under breaking wave contact at 1.2 Hz has also been demonstrated [26]. Consequently, as triboelectricity exists when liquids are flowing or in contact with solid insulated materials [17,27–35], which creates an electric double layer (EDL) in two steps called the Wang model [30,33]. Electron exchange between liquid-solid interface due to contact electrification as the first step that makes the atoms on the solid surface to be ions. The interaction between the solid-liquid interface ions as the second step, resulting in a gradient distribution of cations and anions near the interface [30,33].

* Corresponding author. Mechatronics Research Group, University of Southampton, Southampton, SO17 1BJ, UK.
E-mail addresses: utj1n15@soton.ac.uk (U.T. Jurado); SuanHui.Pu@soton.ac.uk (S.H. Pu); nmw@ecs.soton.ac.uk (N.M. White)

https://doi.org/10.1016/j.nanoen.2020.105204
Received 2 June 2020; Received in revised form 16 July 2020; Accepted 17 July 2020
Available online xxx
2211-2855/

Practically, electron exchange and ion adsorption occur simultaneously and coexist in the liquid-solid interaction [30,32]. Specifically, the contact electrification between hydrophobic surfaces and liquid solutions is more likely to be dominated by electron transfer and the contact electrification between hydrophilic surfaces and liquid solutions is likely dominated by ion transfer [31]. This research work is aimed at an extended experimental study, analysis and optimization to exploit the liquid-solid contact electrification for harvesting breaking wave impact energy, at low frequencies (0.7 Hz–3 Hz). Such energy can be potentially harvested, exploited and improved using a grid of water-dielectric single electrode mode triboelectric nanogenerators (WDSE-TENG). Such an energy harvester converts the external mechanical energy into electricity by a combination of the triboelectric effect and electrostatic induction, based on contact electrification between water and selected hydrophobic dielectric polymer layers due to their high negativity in the triboelectric series [36,37]. Such as polydimethylsiloxane (PDMS, with silicon-oxygen bonds), polytetrafluoroethylene (PTFE, with carbon-fluoride bonds), silicone rubber compound (acetoxy elastomer, with silicon-oxygen bonds), fluorinated ethylene propylene (FEP, with carbon-fluoride bonds) and Polyimide (Kapton, with two acyl groups (C═O), bonded to nitrogen).

First, in order to evaluate the use of water as a triboelectric material for TENG, single-electrode and split-electrode TENG prototypes were fabricated and characterized. The generated output voltage, output current, transferred charge and output power were measured to study the contact electrification between water and the aforementioned dielectric polymer films. Tap water, deionized (DI) water and sodium chloride (NaCl) solution with a concentration of 0.6 M, which is similar to that in seawater, were compared when in contact with the hydrophobic polymer films. This was achieved in a wave tank that generates breaking water wave impacts at frequencies and amplitudes between 0.7 Hz and 3 Hz and 10 cm–12 cm, respectively. The aim was to find the optimum dielectric material to reach the highest output power from the water wave impact. Second, a load resistance matching experiment was performed with the objective being to obtain maximum output power from the WDSE-TENG with a suitable selection of solid materials that gives the highest performance from the proposed prototypes. Third, the produced output performance and ability to charge a variety of capacitors with a single, and also a grid of five, WDSE-TENG prototypes in a multi-unit parallel connection [38–40] to increase the current output were characterized in seawater under breaking water wave impact at the aforementioned frequencies. An enhancement in the performance was achieved using a grid of energy harvesters. Finally, it was demonstrated that the grid of WDSE-TENG has the potential to drive small electronic devices, such as an ultrasonic range sensor for detecting objects during a short period (~1 s). Furthermore, we aim to solve the challenge that this system and many self-powered systems based on TENG have, in that they are not able to work continuously. A power management control circuit (PMCC) was used, which allows the output power performance of the grid of WDSE-TENG to meet the power consumption requirements from 1 mW to 100 mW [41,42] for electronic devices. This demonstrates an alternative and novel approach for energy harvesting of ocean wave impact for autonomous monitoring applications requiring self-powered systems in liquid environments. Potential use cases include systems at structure-water interfaces in aquaculture for fish detection, measurement of the water levels at smart fish farms at small and big scales harvesting breaking water wave energy in areas between ~145 cm^2 to ~18 m^2, and sensor systems that monitor erosion in coastal defence systems.

2. WDSE-TENG prototypes fabrication and electrical characterization measurements set-up

2.1. Fabrication

The fabricated WDSE-TENG prototypes have a triboelectric active area of 7 cm × 4 cm and three different configurations, as depicted in Fig. 1, using hydrophobic dielectric layers with high negativity in the triboelectric series [36]. For the first sample of a WDSE-TENG, a dielectric layer was bonded onto a copper electrode (thickness (t) = 100 μm) with conductive acrylic glue (Electrical resistance through glue = 0.003 Ω, and t = 25 μm). The other exposed side of the copper layer was insulated with black PTFE tape to protect it from the water to prevent a short circuit (Fig. 1 a). With this device configuration, the contact electrification occurs at the face of the dielectric layer in contact with water. A number of different dielectric layers were tested, namely PTFE (t = 100 μm), FEP (t = 25 μm), Silicone rubber compound (t = 150 μm), Kapton (t = 127 μm), and PDMS (t = 125 μm). For the second configuration, a Cu layer (t = 100 μm) was completely insulated within silicone rubber layers on both sides to protect it from the water (Fig. 1 b) and to increase the contact area to produce contact electrification on both faces of the device when water contacts it. Additionally, using the second configuration, a copper layer was insulated on one side with a layer of PDMS and the other side with a layer of PTFE using conductive acrylic adhesive to test the combination of two different materials in contact electrification with water at the same time. For the electrical characterization, the electrode of each sample was connected to an external load of 10 MΩ.

The third configuration comprised two copper layers (split electrode) with an active area of 2.5 cm × 3 cm per layer, and a separation distance of 8 mm, which were bonded with conductive acrylic adhesive on a dielectric layer of either PTFE (t = 100 μm) or PDMS (t = 125 μm). The other face of the device was insulated with a layer of silicone rubber to protect it from short-circuit in contact with water (Fig. 1 c). The contact electrification is produced on both faces of the device when it contacts the water and the two electrodes (E1 and E2) were connected to an external load of 10 MΩ for electrical characterization. The objective of implementing a split electrode design commonly called the free-standing mode [43] is to increase the overall charge transfer relative to a WDSE-TENG.

2.2. Electrical characterization

The WDSE-TENG output voltage, output current, charge transfer and output power of the prototypes were characterized in a breaking water wave generator tank in order to replicate the conditions of the mechanical energy generated by ocean wave impact. A hybrid stepper motor (RS Pro 535-0502) attached with an acrylic panel of 20 cm × 20 cm (t = 8 mm) is used to generate the wave motion in the water tank at different frequencies. The water wave breaks with frequencies from 0.7 Hz to 3 Hz and amplitudes between 10 cm and 12 cm (See Fig. S1 in the supplementary information document). The WDSE-TENG devices were placed at the wall on the right side of the tank where the water wave breaks against the dielectric triboelectric layer, which generates interchange of triboelectric charges between both surfaces as shown in Fig. 2 a and Fig. 2 c. DI water, tap water and 0.6 M NaCl solution (artificial seawater) were used in contact with the WDSE-TENG devices. Therefore, a practical load resistance matching analysis with load resistances varying between 100 Ω and 100 MΩ connected to the energy harvester prototype was performed to obtain the maximum output power as depicted in Fig. 2 b.

Additionally, the rectified output performance and the ability to charge a variety of capacitors varying from 4.7 μF to 470 μF for 85 s with a single device (Fig. 2 a), and a grid of five WDSE-TENG devices

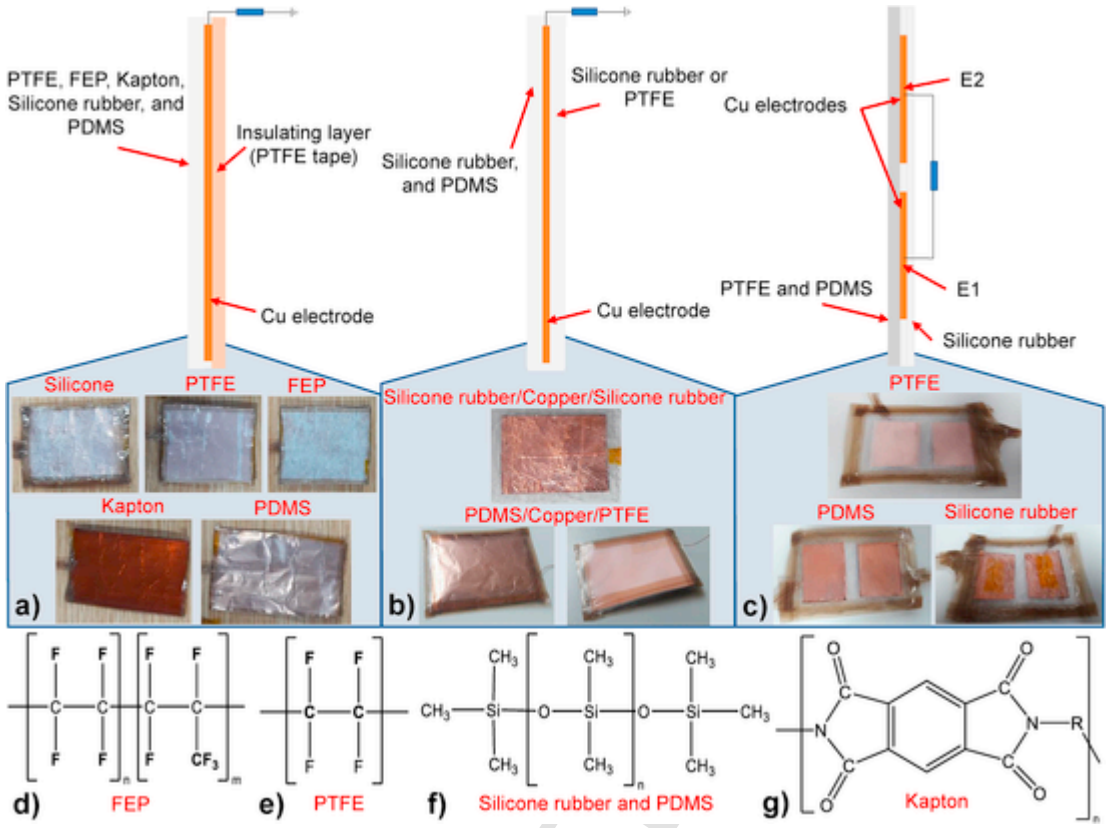

Fig. 1. Two-dimensional schematic and digital images of the three configurations of fabricated WDSE-TENG prototypes a) WDSE-TENG with one dielectric layer, b) full device covered with two dielectric layers and c) split electrode-two dielectric layers. Molecular structure of d) FEP, e) PTFE, f) Silicone rubber (Acetoxy, elastomer) and PDMS and g) Kapton.

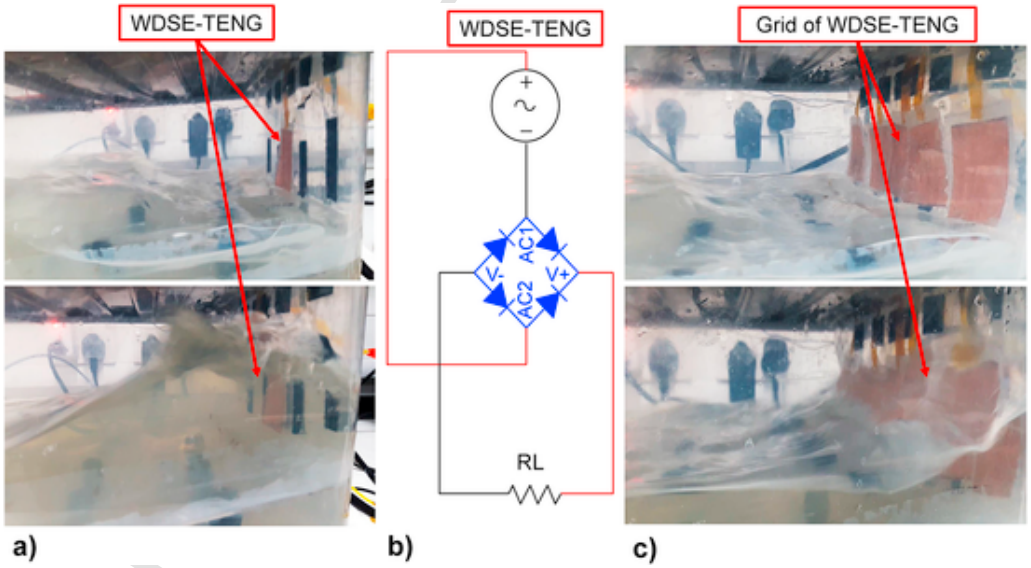

Fig. 2. a) Digital image of the single WDSE-TENG attached and under breaking water wave impact in the water wave impact generator tank. b) Circuit diagram of the WDSE-TENG for the load matching and charging of different capacitors. c) Digital image of the grid of five WDSE-TENG devices attached and under breaking water wave impact in the water wave impact generator tank.

connected in parallel were tested as illustrated in Figs. 2 c and Fig. 10 a. Every WDSE-TENG device was connected to a full wave bridge rectifier (using BAS 40 diodes) for the electrical characterization of the grid of such devices. Furthermore, a durability test was performed to the WDSE-TENG energy harvester under breaking water wave impact through different periods from 30 min to 210 min and number of cycles of operation. Moreover, the grid of energy harvesters was used to drive electronic devices including an HC-SR04 ultrasonic ranger by storing and discharging electrical energy using capacitors. Finally, a PMCC unit was developed using the grid of WDSE-TENG as a source and this improved its energy extraction to have a direct wave impact-to-electrical conversion.

All the WDSE-TENG prototypes and connection wires were insulated to avoid short circuit conditions when the devices are in contact

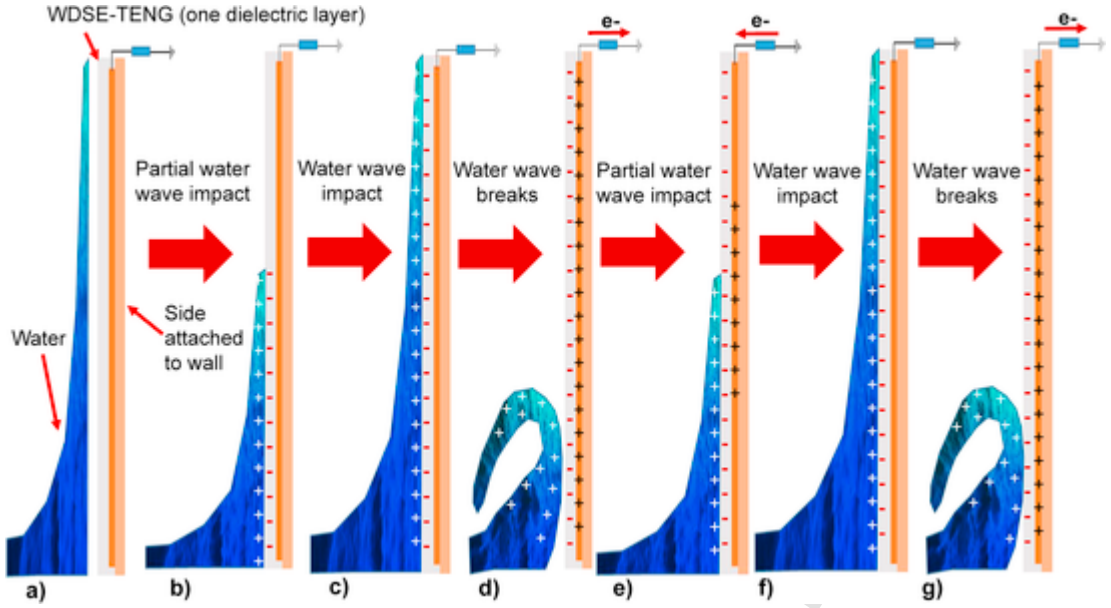

Fig. 3. a–g. Working mechanism of the WDSE-TENG with one-dielectric layer by the contact electrification of dielectric layers with breaking water wave impact.

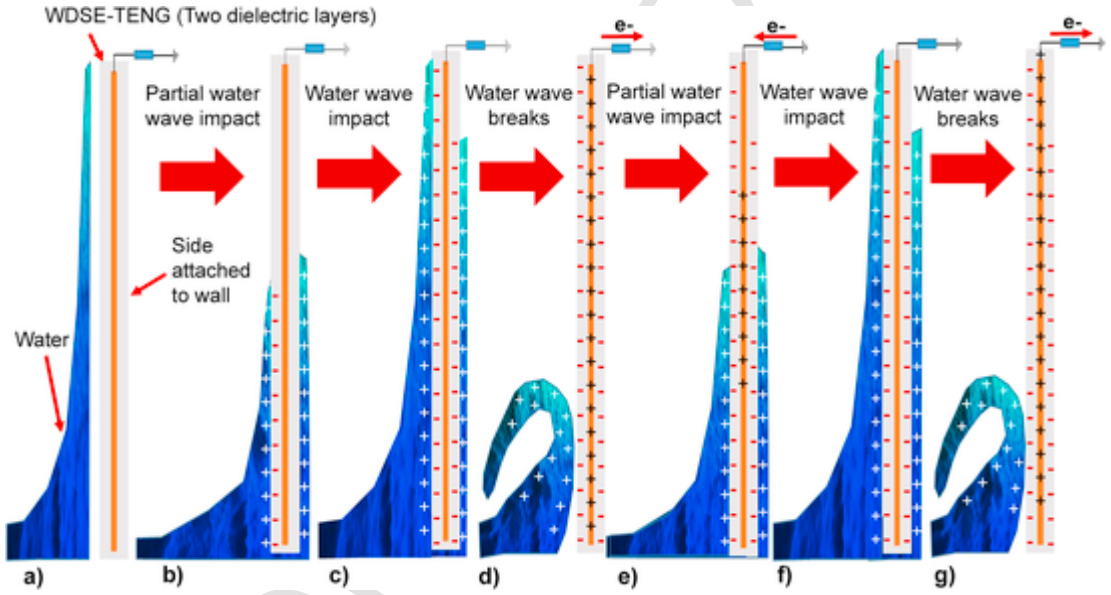

Fig. 4. a–g. Working mechanism of the WDSE-TENG with two-dielectric layers by the contact electrification of dielectric layers with breaking water wave impact.

with water. The output voltage and current measurements of the WDSE-TENG energy harvesters were performed using an Agilent Technologies N6705B Power analyzer (10 measurements performed for each sample). The output power was calculated from these measurements. Furthermore, the transferred charges were calculated by integrating the output current peaks generated during the impact of the water waves over the devices, and the charge of different capacitors (4.7 μF–470 μF) by the energy harvesters were obtained with a Tektronix TDS 2014C digital oscilloscope (10 measurements performed for each sample).

3. WDSE-TENG working mechanism through water-dielectric interfaces for electricity generation

Fig. 3 a-g and Fig. 4 a-g illustrates the working mechanism of the WDSE-TENG with one-dielectric layer and two-dielectric layers configuration due to contact electrification and ion interaction between the breaking water wave and the hydrophobic dielectric layers. Before the dielectric layers make contact with water (Fig. 3 a and Fig. 4 a), no charge transfer and ion adsorption occur. When the water wave starts to make partially contact against the dielectric layers (Fig. 3 b and Fig. 4 b), the electron exchange and ionization of the surface groups on the dielectric layers will cause the dielectric layer to be negatively charged [44] and create a positively charged EDL on the contact surface of the water wave to maintain electrical neutrality [30–33,45,46] (Fig. 3 c and Fig. 4 c). As the water wave breaks down and moves off the dielectric layers, the positive charges in the EDL can be carried away with the water and the negative charges can remain on the surface of the dielectric layers. The negative electric potential difference between the electrode and the load resistor to ground attains equilibrium as electrons flow to ground (Fig. 3 d and Fig. 4 d) due to the triboelectric charges on the dielectric layers, which can be retained for hours or even days [47]. When another water wave is partially impacting/contacting the negatively charged dielectric layers in a short period (~0.0008 s) of the impact motion process (See Fig. S2 in the supplementary information document), the negative charges will attract

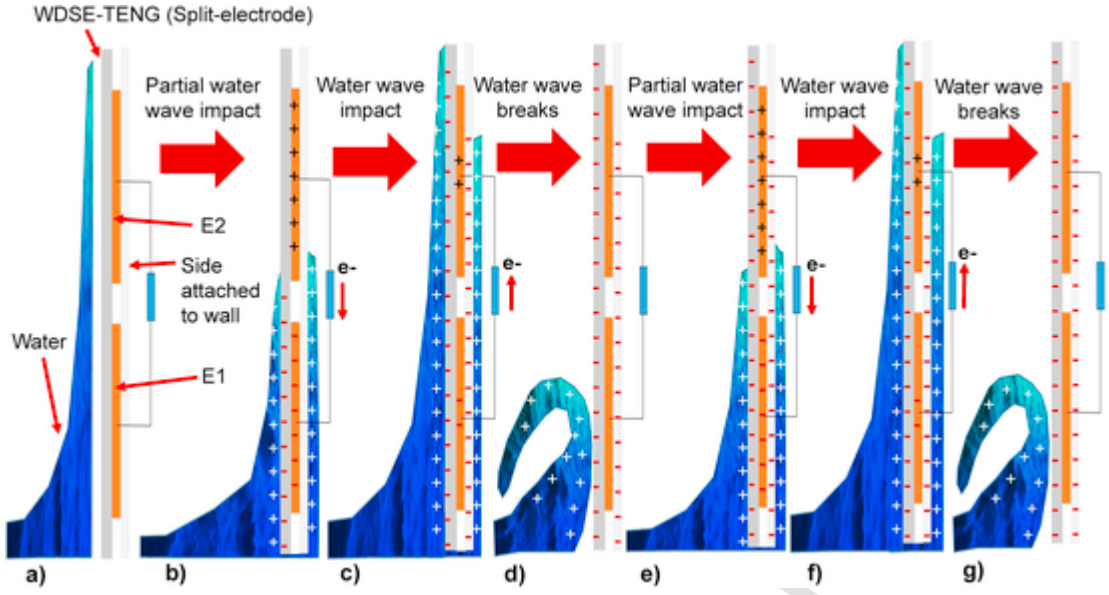

Fig. 5. a–g. Working mechanism of the split-electrode WDSE-TENG with two-dielectric layers by the contact electrification of dielectric layers from breaking water wave impact.

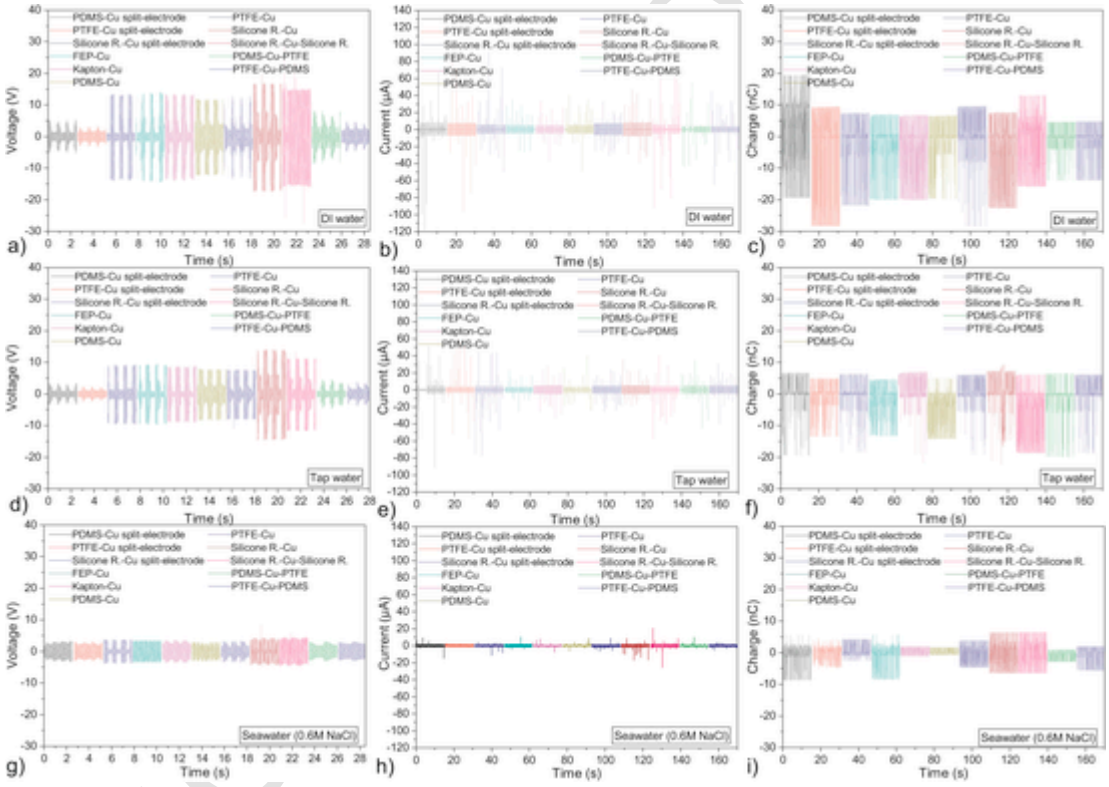

Fig. 6. The average instantaneous output voltage, output current and transferred charges of the WDSE-TENG with different configurations and materials in contact with (a–c) DI water, (d–f) tap water and (g–i) artificial seawater.

counter ions from the water to form another positively charge EDL, and establishes a positive electric potential difference. Therefore, electrons will flow from ground and load resistor to the electrode (Fig. 3e and Fig. 4 e) that produces an instantaneous current peak until a new equilibrium is reached (~0.29 s, Fig. 3 f and Fig. 4 f) (See Fig. S3 in the supplementary information document). When the water wave breaks down (~0.0103 s) and leaves the dielectric layers, a negative electric potential difference will be established between the electrode and load resistor to the ground and another new equilibrium is achieved (Fig. 3 g and Fig. 4 g). Once the following water wave contacts with the dielectric layers of the WDSE-TENG (Fig. 3 a-g and Fig. 4 a-g), power generation cycle repeats itself.

Additionally, the working mechanism of the WDSE-TENG with split-electrode and two-dielectric layers configuration is depicted in Fig. 5 a-g. No charge transfer and ion adsorption take place before the contact electrification between the dielectric layers and water (Fig. 5 a). Subsequently, the water wave starts its contact over the WDSE-TENG, and this results in electrical neutrality with negative charges on the dielectric layer surface, which also creates a positively charged EDL on the water (Fig. 5 b). This generates an unbalanced electric potential differ-

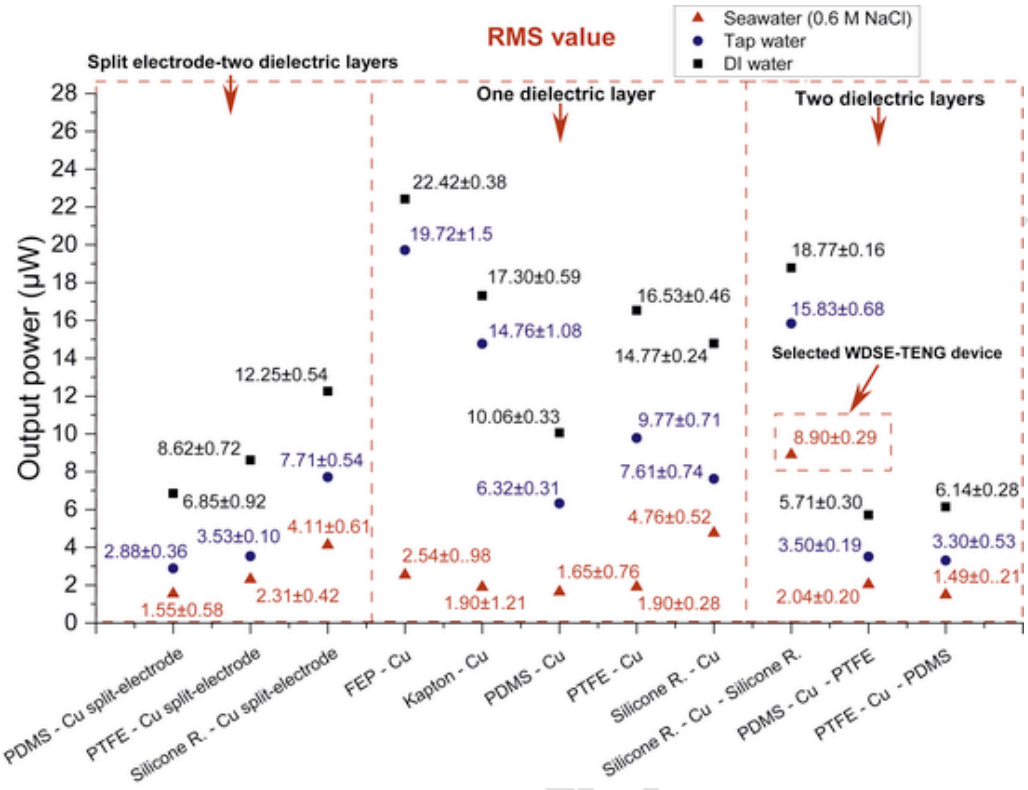

Fig. 7. Comparison of the output power calculated for each of the three WDSE-TENG prototypes when exposed to 10.5 cm amplitude waves at 1.2 Hz (with a 10 MΩ load).

ence between E1 and E2 that drives the movement of electrons from E2, through the load resistance to E1 as the water wave is partially impacting the WDSE-TENG energy harvester (Fig. 5 b). This process produces an instantaneous negative current (Fig. 5 b). Therefore, once the water wave fully impacts the device dielectric layers, induced electrons move back from E1 to E2, through the load resistance as the electric potential distribution changes toward equilibrium which produces an instantaneous positive current (Fig. 5 c). As the water wave breaks down and moves off the dielectric layers, the positive charges in the EDL can be carried away with the water and the negative charges can remain on the surface of the dielectric layers (Fig. 5 d). Once the following water wave starts impacting with the dielectric layers of the split-electrode WDSE-TENG with two-dielectric layers (Fig. 5 e), another cycle of operation is completed (Fig. 5 f-g). The water wave after the impact with the dielectric layers of the WDSE-TENG prototypes should not leave residual water on the dielectric hydrophobic layers surface, in an ideal situation to generate the maximum electrical output.

4. Experimental results and discussion

4.1. Water-dielectric triboelectric materials selection and optimization

The comparison of the three configurations for the WDSE-TENG energy harvester prototypes according to their electrical output performance measurements in contact with DI water, tap water and seawater with a frequency and amplitude of impact of 1.2 Hz and 10.5 cm is shown in Fig. 6 a-i (See Fig. S2 in the supplementary information document). In contact with DI water, the devices had a maximum output voltage (V_{RMS}), output current (I_{RMS}) and transferred charges ranging from 3.06 V to 7.36 V, 1.87 μA–5.06 μA and 5.41 nC–13.70 nC (Fig. 6 a-c), respectively. As a result, a maximum output power between 5.71 μW and 22.42 μW was calculated (Fig. 7). In contact with tap water, the maximum output power was between 2.88 μW and 19.72 μW and this was calculated from the measured V_{RMS} (1.47 V–5.76 V) and I_{RMS} (1.04 μA–4.80 μA), along with transferred charges of 4.98 nC–9.93 nC (Fig. 6 d-f). The output performance using tap water was reduced by a factor of 1.46 compared with the DI water (Fig. 7).

The WDSE-TENG with one dielectric layer using FEP (t = 25 μm) in contact with tap water and DI water produced the highest output performance (Fig. 7). The prototype with two dielectric layers of silicone rubber produced the next highest output performance, likely due to the large contact area (V_{RMS}, I_{RMS} and power of 5.76 V–6.21 V, 2.74 μA–3.04 μA and 15.83 μW–18.77 μW, respectively). However, the output performance decreased for the WDSE-TENG with split-electrode with two dielectric layers due to the reduced active area of 2.5 cm × 3 cm. Furthermore, the configuration of the WDSE-TENG with two distinct dielectric layers of PDMS and PTFE have shown relatively poor output power performance from 3.30 μW to 6.14 μW (Fig. 7).

Moreover, the output power for the water-dielectric energy harvesters was reduced by a factor of 4.20 and 2.86 when they were in contact with seawater compared with the DI and tap water, respectively (Fig. 7). The maximum output voltage, current, transferred charge and output power values were 3.75 V, 2.37 μA, 4.63 nC and 8.89 μW with the two dielectric layer configuration using silicone rubber compound (t = 150 μm) with a Cu electrode as depicted in Fig. 6 g-i and Fig. 7. For the one dielectric layer configuration using silicone rubber, a maximum output power of 4.76 μW (Fig. 7) was obtained, with corresponding output voltage, current and transferred charge values of 4.93 V, 0.96 μA and 3.98 nC, respectively. The reduction in the performance of the WDSE-TENG energy harvesters indicated that they are affected by the electrolytes in water. This is due to the fact that dielectric materials cannot completely elude the adhesion of water droplets after it is separated from the water wave impact. Once there are electrolytes in water, more positive charges including dissolved ions will remain on the dielectric films, resulting in the partial screening of the tribo-charges on the films [36,44,48–51]. In the near future, this issue could be solved by the creation of superhydrophobic dielectric

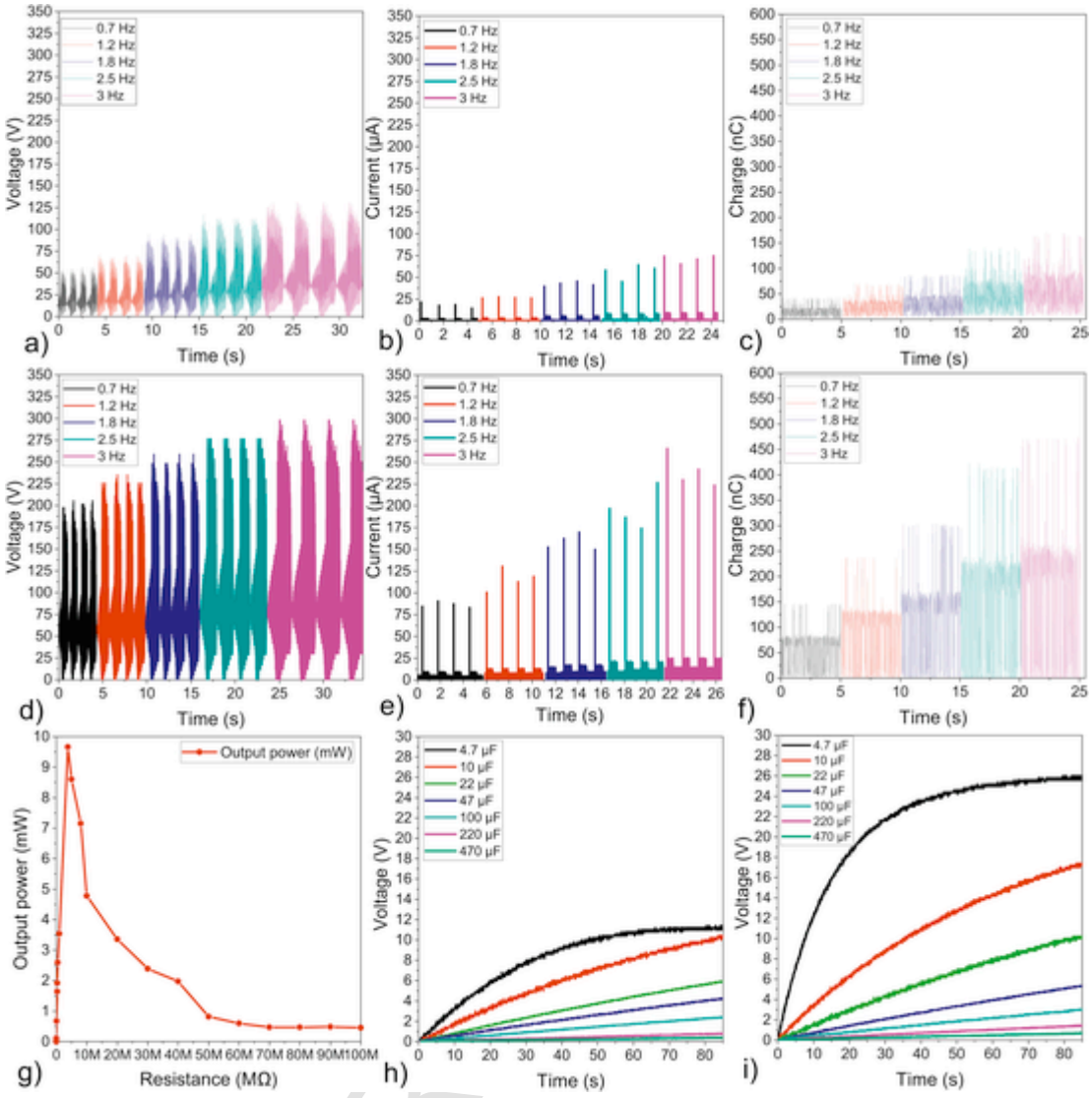

Fig. 8. a) Instantaneous output voltage, b) current and c) transferred charges of a single WDSE-TENG with two-dielectric layers of silicone rubber compound. d) Instantaneous output voltage, e) current and f) transferred charges of the grid of five WDSE-TENG devices through different breaking wave impact frequencies (0.7 Hz–3 Hz) with a load resistance of 3.8 MΩ. g) Load resistance matching analysis to obtain the highest output power performance with the WDSE-TENG devices. h) Charging performance of a single WDSE-TENG energy harvester, and i) a grid of five WDSE-TENG energy harvesters connected in parallel to different capacitors (4.7 μF–470 μF) tested in the water generator tank.

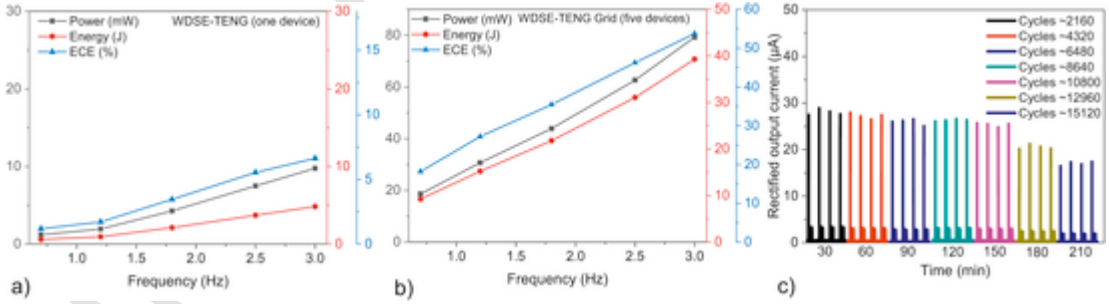

Fig. 9. a) Average instantaneous output power, energy and energy conversion efficiency of a single WDSE-TENG with two-dielectric layers of silicone rubber compound over 15 seconds. b) Average instantaneous output power, energy and energy conversion efficiency of the grid of five WDSE-TENG devices through different breaking wave impact frequencies (0.7 Hz–3 Hz) and amplitudes (10 cm–12 cm) with a load resistance of 3.8 MΩ, for 15 s. c) Maximum average instantaneous output current generated by the WDSE-TENG during different periods and cycles of operation from 30 min to 210 min and ~2160 cycles to ~15120 cycles under breaking water wave impact.

layers or by changing the dielectric film with a specific functional group to counter the ions with opposite charges that remain on the contacted surfaces [49] during water wave impact.

The results show that the reduction in the performance of the WDSE-TENG can be compensated by increasing the contact area of the devices operating with seawater to obtain a better output performance (Fig. 7). Consequently, as the WDSE-TENG energy harvesters must be

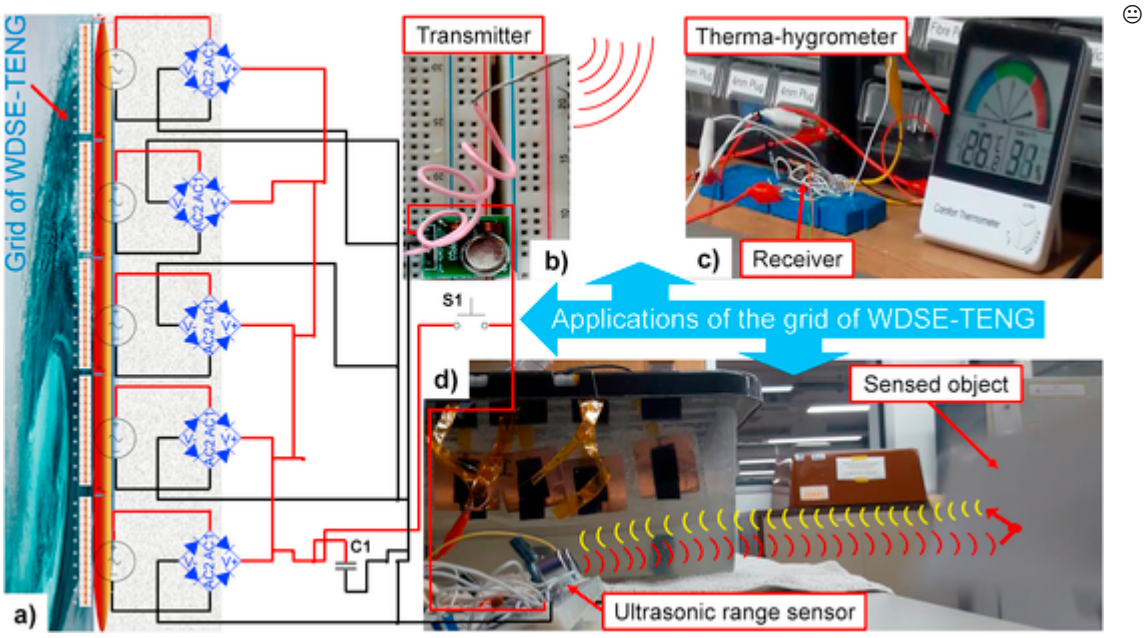

Fig. 10. a) Electrical circuit diagram of the grid of WDSE-TENG energy harvesters under breaking water wave impact to charge the 47 μF and 470 μF capacitors to power-up b) the wireless transmitter to turn on c) a therma-hygrometer and d) an ultrasonic range sensor (Ocean water wave adapted from Ref. [59]).

working in seawater conditions under breaking water wave impact, the selected devices for further characterization were the ones composed with two dielectric layers composed of silicone rubber (Fig. 7. The selected devices generated the highest power performance of 8.90 μW under seawater conditions due to the effective contact area of 46 cm^2 (Fig. 1 b), compared with the other energy harvesters with active areas of 28 cm^2 and 27.2 cm^2 (Fig. 1 a and 1 c). The performance of the triboelectric liquid-solid interfaces used for the WDSE-TENG energy harvesters, arranged according to the output performance under breaking water wave impact is summarized in Table 1. The most negative material generating significant electron transfer effect in contact with DI water and tap water was FEP (See Table S1 in the supplementary information document). On the contrary, the most negative dielectric material with the seawater-dielectric interface interaction was Silicone rubber compound (Fig. 7), which means that the charge transferred using this water-dielectric interface is the highest from the selected triboelectric materials, with the objective being to reach the highest electric output performance in the proposed WDSE-TENG energy harvesters in seawater conditions. Nevertheless, the WDSE-TENG devices comprising FEP, PTFE, Polyimide and PDMS layers in contact with seawater show weak electron transfer effect, which means that ion adsorption effect dominates the contact electrification with those polymers [34,35].

Table 1
Comparison of the level of positive and negative triboelectric water-dielectric interfaces in terms of ease of losing or gaining electrons through breaking seawater wave impact.

Triboelectric liquid-solid interfaces combination		
Liquid	Positive	DI water Tap water Seawater (0.6M NaCl)
Solid	Negative	Polydimethylsiloxane (PDMS) (125 μm) Polyimide (127 μm) Polytetrafloroethylene (PTFE) (100 μm) Fluorinated ethylene propylene (FEP) (24 μm) Silicone rubber compound (Acetoxy, Elastomer) (150 μm)

4.2. Grid/single WDSE-TENG output performance electrical characterization under different breaking water wave impact frequencies and potential battery-less applications

The WDSE-TENG with two-dielectric layers comprising silicone rubber compound exhibit maximum output power and power density of 9.65 mW and 0.21 mW/cm^2, respectively. These values were obtained with a load resistance of 3.8 MΩ, selected from a load resistance matching characterization under breaking water wave impact at 3 Hz with an amplitude of 12 cm (Fig. 8 g). Further, the grid/single WDSE-TENG tested in seawater through different breaking water wave impact frequencies (0.7 Hz–3 Hz) and amplitudes (10 cm–12 cm) show a linear increase in their overall output performance by a factor of 3.29 and 2.54 as the frequency of impact increases as illustrated in Fig. 8 a-f (See Table S2 in the supplementary information document). Such increase is attributed and proportional to the total mechanical energy of the breaking water wave impact (2) consisting of potential and kinetic energy that contacts on the WDSE-TENG devices. Which rises from 50.76 J to 73.10 J that produces an increase in the friction between the liquid-solid interface [35,52–54] (Fig. 4 e) increasing the electron exchange and ion adsorption that occurs simultaneously [30–33] as the frequency and amplitude of impact rises (See Fig. S4 in the supplementary information document). The maximum rectified output power of the single WDSE-TENG device increases from 1.21 mW to 9.76 mW (Fig. 9 a-b), with corresponding maximum instantaneous output voltage, current and transferred charge values of 56.84 V–130 V, 21.31 μA–74.67 μA and 41.79 nC–169 nC, respectively (Fig. 8 a-c).

In comparison, the grid of five energy harvesters connected in parallel, with a total active area of 230 cm^2, showed an overall enhancement by a factor of 6.14 in the average rectified instantaneous output performance with an increasing output voltage, current and transferred charges from 205.63 V to 298 V, 90.52 μA–265.78 μA and 144.9 nC–469.70 nC, respectively (Fig. 8 d-f). Consequently, the grid of energy harvesters generated a maximum output power and power density of 18.61 mW–79.18 mW (Fig. 9 a-b) and 0.081 mW/cm^2 to 0.344 mW/cm^2 (3.8 MΩ load). Furthermore, the output performance enhancement was verified by charging different capacitors

(4.7 μF–470 μF). The maximum voltage reached by the single unit of WDSE-TENG was 11.18 V, compared with the grid of WDSE-TENG devices that reached a maximum value of 25.73 V, when charging a capacitor of 4.7 μF for 85 s as illustrated in Fig. 8 h and Fig. 8 i.

Additionally, the average energy conversion efficiency (ECE) η of one WDSE-TENG energy harvester and a grid of WDSE-TENG composed of five devices was calculated. The ECE is defined as the ratio between the electric energy ($E_{electric}$) delivered to the load resistor of 3.8 MΩ and the mechanical energy ($E_{waterwave}$) applied by the breaking water wave impact on the single/grid of WDSE-TENG devices. A time period of 15 s was considered when calculating $E_{electric}$ for different frequencies (0.7 Hz–3 Hz) and amplitudes (10 cm–12 cm). The $E_{electric}$ released for the single and grid WDSE-TENG energy harvesters were from 0.6 J to 4.84 J and 9.23 J–39.28 J, respectively as shown in Fig. 9 a-b. These values were estimated using the following equation:

$$E_{electric} = \int_{t1}^{t2} RI^2 dt \quad (1)$$

where I is the average instantaneous current generated by the devices and R is the load resistance. The total mechanical energy of the water waves was between 50.76 J and 73.10 J consisting of potential energy and kinetic energy [55]:

$$E_{waterwave} = \frac{1}{2}\rho g A^2 \quad (2)$$

Where g is the acceleration of gravity, ρ is the density of seawater (1036 kg/m^3) [56], and A is the wave amplitude (from 10 cm to 12 cm. Consequently, the overall η of the single/grid of WDSE-TENG energy harvesters rise linearly between 1.18% and 6.62% and 18.19% and 53.74% as depicted in Fig. 9 a-b, calculated by Ref. [57]:

$$\eta = \frac{E_{electric}}{E_{waterwave}} x100\% \quad (3)$$

Moreover, analyzing the potential to scale up the energy harvesting of breaking water wave on an area of 18 m^2, where the water wave breaks with amplitudes between 0.3 m and 4 m [58] using a grid of WDSE-TENG. This could be possible with the fabrication of big water-dielectric triboelectric-structure interfaces composed with 7200 energy harvesters connected in parallel, which could have the potential to generate an average output power, and energy of ~30.63 W and ~15.20 kJ, respectively. Consequently, estimating the breaking of a water wave with an amplitude of 4 m that generates the energy of 78.4 kJ (2) impacting over the big proposed interface. The big-scale grid of WDSE-TENG could have an ECE of 19.38% (3), collecting breaking water wave impacts in big-scale with different amplitudes in the aforementioned area. Besides, a durability test was performed on the WDSE-TENG device composed of two silicone rubber dielectric layers under breaking water wave impact with a frequency and amplitude of ~1.2 Hz and ~10.5 cm, over different periods of 30, 60, 90, 120, 150 and 180 min. Based on the number of cycles of operation and the rectified output current of the WDSE-TENG energy harvester. The results show that the energy harvester maximum average output current is stable over 150 min and ~10800 cycles of operation under the impact of water waves as illustrated in Fig. 9 c. Subsequently, the performance decreases linearly as the operation time increases from 150 min to 180 min and 210 min with a decrease by a factor of 1.27 and 1.55, respectively (Fig. 9 c). The average maximum instantaneous current decreased from ~27.14 μA (60–150 min) to ~21.21 μA and ~17.41 μA (180–210 min) as the cycle of operation increases from ~12960 to ~15120, respectively. Although under ~10800 cycles of operation, the WDSE-TENG performance was stable, further investigation is required to improve the energy conversion efficiency and device durability to withstand the harsh environmental conditions of the ocean and liquid environments.

Besides, due to the improvement of the breaking water wave energy harvesting through the implementation of the grid of WDSE-TENG devices charging different capacitors (Fig. 10 a), some applications were demonstrated. First, the grid of WDSE-TENG energy harvesters was used to power a one way wireless 433 MHz transmitter (Seeed Studio RF link kit part no. 113990010) to send a signal to the receiver to turn on a therma-hygrometer with a transmission distance from 2 m to 8 m as shown in Fig. 10 b-c. This was achieved after charging a 47 μF capacitor between 129 and 370 s, resulting in a voltage of 3.19 V–9.81 V across the capacitor, and then using the stored electrical energy to power up the transmitter. To transmit at longer distances, more energy can be stored by charging suitable capacitors for a longer time. The energy stored in the capacitor for the grid of WDSE-TENG devices, and the power generated for the capacitor during the discharging process for powering the wireless transmitter were between 193.56 μJ and 2.24 mJ, and 322 μW to 3.73 mW, respectively (Fig. 11 a and Fig. 11 c).

Furthermore, an ultrasonic range sensor (HC-SR04) for detection of objects was powered by charging a 470 μF capacitor for 570 s (Figs. 10 d and Fig. 11 b) using the grid of energy harvesters. The range sensor was able to track the movement of a plastic sheet located at a distance of ~30 cm over a short period (~1 s) as illustrated in Fig. 10 d. The energy stored in the capacitor for the grid of energy harvesters and the power supplied by the capacitor to power up the ultrasonic ranger sensor were 5.96 mJ and 5.18 mW, respectively. This demonstration confirmed that the grid of energy harvesters using a liquid-solid interface was able to drive typical electronic devices found in wireless sensor systems.

Finally, energy transfer with a pre-storage capacitor (Ct) was used to store the energy from the grid of WDSE-TENG and to maintain the optimal voltage across the diode rectifier bridge in order to optimize energy extraction. This was achieved using a flyback converter circuit that gives more design flexibility [60]. Therefore, a LT8303 micropower high-voltage insolated flyback converter was integrated to the grid of WDSE-TENG to form a power management control circuit (PMCC) [60] as shown in Fig. 11 d-e. The objective of the PMCC is to maintain the voltage constant across the diode rectifier, when the temporary capacitor (4.7 μF) reaches approximately 5 V after 12.8 s (Fig. 11 f). This is achieved by transferring one part of the energy stored in Ct to the storage capacitor (Cs, 100 μF) through the flyback converter (Fig. 11 f). Harvesting the breaking water wave impact for 200 s, the storage capacitor reached a maximum voltage of 2.64 V with a stored energy of 16.37 μJ, as shown in Fig. 11 f. This power conversion principle enables the utilization of multiple WDSE-TENG connected in parallel using one coupled inductor and only one PMCC (Fig. 11 d-e). This system is able to improve the output power of the water-dielectric energy harvesters with the potential to power up electronic devices such as autonomous wireless sensor nodes for detecting fish and measuring water levels at smart fish farms.

5. Conclusions

In summary, this research work has demonstrated the potential of WDSE-TENG devices as an innovative and alternative approach for harvesting mechanical energy from breaking wave impact forces at the structure-water interfaces using water as a triboelectric material. This contributes to existing energy harvesting studies that are focused on shallow water wave energy harvesting employing liquid-solid interfaces [3–21].

Firstly, by comparing WDSE-TENG composed of different device configurations and five hydrophobic dielectric materials in contact with DI water, tap water and seawater, the ideal energy harvester configuration and the liquid-solid interface was found in order to enhance the output performance of the proposed energy harvesters. The performance of the DI/tap water-FEP WDSE-TENG were the most promising.

Fig. 11

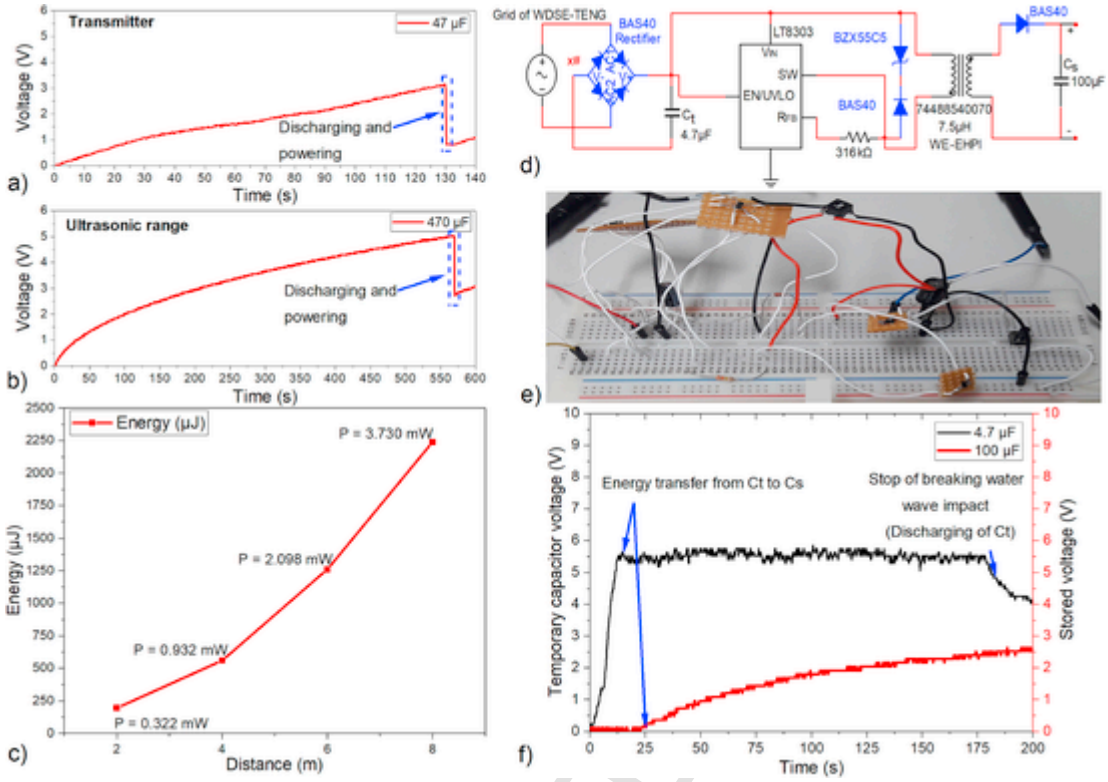

Capacitor charging and discharging process for powering the a) wireless transmitter to power-up the therma-hygrometer, and b) ultrasonic range sensor under the breaking water wave impact with a frequency of 1.2 Hz. c) Energy stored in the 47 μF capacitor for the grid of WDSE-TENG devices, and the power supplied by the capacitor during the discharging process for powering the wireless transmitter to turn on a therma-hygrometer. d) Integration of the grid of WDSE-TENG with an LT8303 micropower high-voltage insolated flyback converter to form a power management control circuit (PMCC). e) Digital image of the PMCC circuit with the grid of WDSE-TENG. f) Energy transfer from Ct to Cs from harvesting the breaking water wave impact for 200 s.

On the other hand, a reduction in the performance of the WDSE-TENG with seawater-dielectric interfaces was observed, but it was demonstrated that this can be compensated by increasing the contact area of the devices to enhance the output performance. Consequently, the WDSE-TENG energy harvester comprising two-hydrophobic silicone rubber compounds showed the highest electrical output working in seawater conditions under breaking water wave impact. Secondly, it was demonstrated that an improvement in the power output by a factor of 6.14 for the seawater-dielectric energy harvesters was possible. This was achieved using a parallel connection of a grid of five WDSE-TENG devices with a coverage area of 230 cm^2 compared to a single WDSE-TENG device. The ability to charge different capacitors was demonstrated, and the output voltage, current, transferred charges, output power and ECE values respond with linear and proportional increase as the water wave impact energy rises, increasing the liquid-solid interface friction, electron exchange and ion adsorption [30–33,35,52–54] as the frequency varies from 0.7 Hz to 3 Hz, with amplitudes between 10 cm and 12 cm.

Thirdly, the grid of WDSE-TENG devices has the potential to drive low-power electronic devices with stored energy levels between 2.24 mJ and 5.96 mJ, and they generate power in the range 3.73 mW–5.18 mW, which is sufficient to power an ultrasonic range sensor, and also to power a wireless transmitter. Finally, the integration of the grid of WDSE-TENG devices with a PMCC allows the device to achieve power levels from 1 mW to 100 mW [41,42] for powering electronic devices continuously using a TENG. Further investigation is required to explore the integration of superhydrophobic materials, surface patterning modification to enhance hydrophobicity, utilization of normalized thickness values, and more efficient energy coupling to withstand the seawater conditions utilizing the WDSE-TENG energy harvesters that have a stable electrical output under ~10800 cycles of operation during 150 min, measured through a durability test. The integration of the grid of WDSE-TENG offers an innovative approach that is able to work in liquid environments and hence provide an energy source for self-powered wireless sensing systems at water-structure interfaces. Potential applications include fish detection for smart aquaculture, water level measurements, weather condition monitoring, and sensor systems that monitor erosion and weathering in coastal defence systems.

CRediT authorship contribution statement

Ulises Tronco Jurado: Conceptualization, Methodology, Software, Investigation, Validation, Data curation, Formal analysis, Writing - original draft, Writing - review & editing, Visualization, Project administration. **Suan Hui Pu:** Resources, Conceptualization, Writing - review & editing, Supervision. **Neil M. White:** Resources, Conceptualization, Writing - review & editing, Supervision.

Declaration of competing interest

The authors declare that they have no known competing financial interests or personal relationships that could have appeared to influence the work reported in this paper.

Acknowledgments

The authors thank CONACYT for the fellowship awarded to Ulises Tronco Jurado.

Appendix A. Supplementary data

Supplementary data to this article can be found online at https://doi.org/10.1016/j.nanoen.2020.105204.

References

[1] N Elvin, A Erturk, Advances in Energy Harvesting Methods, Springer Science & Business Media, 2013.
[2] D Jiang, et al., Water-solid triboelectric nanogenerators: an alternative means for harvesting hydropower, Renew. Sustain. Energy Rev. 115 (2019) 109366.
[3] Y Wu, et al., A teeterboard-like hybrid nanogenerator for efficient harvesting of low-frequency ocean wave energy, Nano Energy 67 (2020) 104205.
[4] L Feng, et al., Hybridized nanogenerator based on honeycomb-like three electrodes for efficient ocean wave energy harvesting, Nano Energy 47 (2018) 217–223.
[5] F-R Fan, Z-Q Tian, Z L Wang, Flexible triboelectric generator, Nano energy 1 (2) (2012) 328–334.
[6] G Zhu, et al., Toward large-scale energy harvesting by a nanoparticle-enhanced triboelectric nanogenerator, Nano Lett. 13 (2) (2013) 847–853.
[7] T X Xiao, et al., Spherical triboelectric nanogenerators based on spring-assisted multilayered structure for efficient water wave energy harvesting, Adv. Funct. Mater. 28 (35) (2018) 1802634.
[8] M Xu, et al., High power density tower-like triboelectric nanogenerator for harvesting arbitrary directional water wave energy, ACS Nano 13 (2) (2019) 1932–1939.
[9] S L Zhang, et al., Rationally designed sea snake structure based triboelectric nanogenerators for effectively and efficiently harvesting ocean wave energy with minimized water screening effect, Nano Energy 48 (2018) 421–429.
[10] F Xi, et al., Self-powered intelligent buoy system by water wave energy for sustainable and autonomous wireless sensing and data transmission, Nano Energy 61 (2019) 1–9.
[11] X Yang, et al., Macroscopic self-assembly network of encapsulated high-performance triboelectric nanogenerators for water wave energy harvesting, Nano Energy 60 (2019) 404–412.
[12] B K Yun, H S Kim, Y J Ko, G Murillo, J H Jung, Interdigital electrode based triboelectric nanogenerator for effective energy harvesting from water, Nano Energy 36 (2017) 233–240.
[13] X Yang, S Chan, L Wang, W A Daoud, Water tank triboelectric nanogenerator for efficient harvesting of water wave energy over a broad frequency range, Nano Energy 44 (2018) 388–398.
[14] J-W Lee, W Hwang, Theoretical study of micro/nano roughness effect on water-solid triboelectrification with experimental approach, Nano Energy 52 (2018) 315–322.
[15] X J Zhao, S Y Kuang, Z L Wang, G Zhu, Highly adaptive solid–liquid interfacing triboelectric nanogenerator for harvesting diverse water wave energy, ACS Nano 12 (5) (2018) 4280–4285.
[16] X Li, J Tao, X Wang, J Zhu, C Pan, Z L Wang, Networks of high performance triboelectric nanogenerators based on liquid–solid interface contact electrification for harvesting low-frequency blue energy, Adv. Energy Mater. 8 (21) (2018) 1800705.
[17] Z H Lin, G Cheng, L Lin, S Lee, Z L Wang, Water–solid surface contact electrification and its use for harvesting liquid-wave energy, Angew. Chem. Int. Ed. 52 (48) (2013) 12545–12549.
[18] L Pan, et al., Liquid-FEP-based U-tube triboelectric nanogenerator for harvesting water-wave energy, Nano Res. 11 (8) (2018) 4062–4073.
[19] G Zhu, et al., Harvesting water wave energy by asymmetric screening of electrostatic charges on a nanostructured hydrophobic thin-film surface, ACS Nano 8 (6) (2014) 6031–6037.
[20] B Zhang, et al., Self-powered acceleration sensor based on liquid metal triboelectric nanogenerator for vibration monitoring, ACS Nano 11 (7) (2017) 7440–7446.
[21] X Zhang, et al., Self-powered distributed water level sensors based on liquid–solid triboelectric nanogenerators for ship draft detecting, Adv. Funct. Mater. 29 (41) (2019) 1900327.
[22] R B Mayon, Investigation of Wave Impacts on Porous Structures for Coastal Defences Doctoral University of Southampton, 2017 [Online]. Available https://eprints.soton.ac.uk/422221/.
[23] U T Jurado, S H Pu, N M White, A contact-separation mode triboelectric nanogenerator for ocean wave impact energy harvesting, 2017 IEEE SENSORS, IEEE, 2017, pp. 1–3.
[24] U T Jurado, S H Pu, N M White, Dielectric-metal triboelectric nanogenerators for ocean wave impact self-powered applications, IEEE Sensor. J. 19 (16) (2019) 6778–6785.
[25] U T Jurado, S H Pu, N M White, Grid of hybrid nanogenerators for improving ocean wave impact energy harvesting self-powered applications, Nano Energy 72 (2020) 104701.
[26] U T Jurado, S H Pu, N M White, Water-dielectric single electrode mode triboelectric nanogenerators for ocean wave impact energy harvesting, Multidiscipl. Dig. Publ. Inst. Proc. 2 (13) (2018) 714.
[27] B Ravelo, F Duval, S Kane, B Nsom, Demonstration of the triboelectricity effect by the flow of liquid water in the insulating pipe, J. Electrost. 69 (6) (2011) 473–478.
[28] Y Sun, X Huang, S Soh, Using the gravitational energy of water to generate power by separation of charge at interfaces, Chem. Sci. 6 (6) (2015) 3347–3353.
[29] U Khan, S-W Kim, Triboelectric nanogenerators for blue energy harvesting, ACS Nano 10 (7) (2016) 6429–6432.
[30] Z L Wang, Triboelectric nanogenerator (TENG)—sparking an energy and sensor revolution, Adv. Energy Mater. 10 (17) (2020) 2000137.
[31] S Lin, L Xu, A C Wang, Z L Wang, Quantifying electron-transfer in liquid-solid contact electrification and the formation of electric double-layer, Nat. Commun. 11 (1) (2020) 1–8.
[32] L Zhou, D Liu, J Wang, Z L Wang, Triboelectric nanogenerators: fundamental physics and potential applications, Friction (2020) 1–26.
[33] Z L Wang, A C Wang, On the origin of contact-electrification, Mater. Today 30 (2019) 34–51.
[34] J Nie, et al., Probing contact-electrification-induced electron and ion transfers at a liquid–solid interface, Adv. Mater. 32 (2) (2020) 1905696.
[35] S Li, et al., Contributions of different functional groups to contact electrification of polymers, Adv. Mater. 32 (25) (2020) 2001307.
[36] A Diaz, R Felix-Navarro, A semi-quantitative tribo-electric series for polymeric materials: the influence of chemical structure and properties, J. Electrost. 62 (4) (2004) 277–290.
[37] D Davies, Charge generation on dielectric surfaces, J. Phys. Appl. Phys. 2 (11) (1969) 1533.
[38] Z L Wang, T Jiang, L Xu, Toward the blue energy dream by triboelectric nanogenerator networks, Nano Energy 39 (2017) 9–23.
[39] L Xu, et al., Coupled triboelectric nanogenerator networks for efficient water wave energy harvesting, ACS Nano 12 (2) (2018) 1849–1858.
[40] J Chen, et al., Networks of triboelectric nanogenerators for harvesting water wave energy: a potential approach toward blue energy, ACS Nano 9 (3) (2015) 3324–3331.
[41] D Steingart, Power sources for wireless sensor networks, Energy Harvesting Technologies, Springer, 2009, pp. 267–286.
[42] Z L Wang, W Wu, Nanotechnology-enabled energy harvesting for self-powered micro-/nanosystems, Angew. Chem. Int. Ed. 51 (47) (2012) 11700–11721.
[43] Z L Wang, L Lin, J Chen, S Niu, Y Zi, Triboelectric nanogenerator: freestanding triboelectric-layer mode, Triboelectric Nanogenerators, Springer, 2016, pp. 109–153.
[44] D Choi, H Lee, I S Kang, G Lim, D S Kim, K H Kang, Spontaneous electrical charging of droplets by conventional pipetting, Sci. Rep. 3 (2013) 2037.
[45] J Lyklema, Fundamentals of Interface and Colloid Science: Soft Colloids, Elsevier, 2005.
[46] Z H Lin, G Cheng, S Lee, K C Pradel, Z L Wang, Harvesting water drop energy by a sequential contact-electrification and electrostatic-induction process, Adv. Mater. 26 (27) (2014) 4690–4696.
[47] Y Tada, Experimental characteristics of electret generator, using polymer film electrets, Jpn. J. Appl. Phys. 31 (3R) (1992) 846.
[48] B J Kirby, E F Hasselbrink Jr., Zeta potential of microfluidic substrates: 1. Theory, experimental techniques, and effects on separations, Electrophoresis 25 (2) (2004) 187–202.
[49] L S McCarty, G M Whitesides, Electrostatic charging due to separation of ions at interfaces: contact electrification of ionic electrets, Angew. Chem. Int. Ed. 47 (12) (2008) 2188–2207.
[50] W Harper, Contact and Frictional Electrification, Morgan Hill, Laplacian Press, 1998.
[51] Y Awakuni, J Calderwood, Water vapour adsorption and surface conductivity in solids, J. Phys. Appl. Phys. 5 (5) (1972) 1038.
[52] L Zhao, J Sun, X Wang, L Zeng, C Wang, Y Tu, System-size effect on the friction at liquid-solid interfaces, Appl. Math. Mech. 41 (3) (2020) 471–478.
[53] F-C Wang, Y-P Zhao, Slip boundary conditions based on molecular kinetic theory: the critical shear stress and the energy dissipation at the liquid–solid interface, Soft Matter 7 (18) (2011) 8628–8634.
[54] Y Zhang, et al., Combined effects of pinning and adhesion force on solid\liquid interfacial friction behaviors under applied voltage, Tribol. Int. 134 (2019) 102–108.
[55] A Khaligh, O C Onar, Energy Harvesting: Solar, Wind, and Ocean Energy Conversion Systems, CRC press, 2009.
[56] R Pawlowicz, Key physical variables in the ocean: temperature, salinity, and density, Nat. Educ. Knowl. 4 (4) (2013) 13.
[57] W Tang, et al., Liquid-metal electrode for high-performance triboelectric nanogenerator at an instantaneous energy conversion efficiency of 70.6%, Adv. Funct. Mater. 25 (24) (2015) 3718–3725.
[58] Oceanweathercom Current Marine DataOceanweather Inc, [Online]. Availablehttp://www.oceanweather.com/data/index.html30 October 2018
[59] E. Arano Ocean water wave photo[Online]. Availablehttps://www.pexels.com/photo/ocean-water-wave-photo-1295138/2016
[60] S Boisseau, G Despesse, B A Seddik, Electrostatic conversion for vibration energy harvesting, Small-Scale Energy Harvest. (2012) 1–39.

Biography

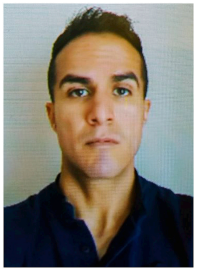

Ulises Tronco Jurado received the M.Sc. degree in materials science from University of Guadalajara, Mexico, in 2015. He was a MEMS lab researcher at the University of Texas at San Antonio, U.S., in 2014, working on modelling, synthesis, fabrication and characterization of quantum dots applied to c-silicon solar cells. He is currently pursuing a PhD. Degree in Engineering and the Environment with the Mechatronics Research Group, and the Smart Electronic Materials and Systems Research Group, School of Electronics and Computer Science, University of Southampton, U.K. His current research interest includes triboelectric nanogenerators for ocean wave monitoring applications that required self-powering.

Suan Hui Pu received Ph.D. degree in electrical and electronic engineering from Imperial College London, U.K. in 2010. He is currently an Associate Professor at University of Southampton at Johor, Malaysia. He is a visiting academic in the Schools of Engineering, and Electronics and Computer Science, at the University of Southampton, U.K. His current research interests include NEMS/MEMS sensors and actuators, graphene/graphite sensors and printed electronics. He has served as a reviewer for IEEE Journal of Microelectromechanical Systems, IEEE Electron Device Letters, IEEE Transactions on Components, Packaging and Manufacturing Technology, IOP Nanotechnology, IOP Journal of Micromechanics and Microengineering, amongst others.

Neil M. White obtained a PhD from the University of Southampton in 1988. Neil was promoted to Senior Lecturer in 1999. His research interests include thick-film sensors, intelligent instrumentation, MEMS, self-powered microsensors and sensor networks. He is a Chartered Engineer, Senior Member of the IEEE, and a Chartered Physicist. He is a member of the Peer Review College for the EPSRC and is on the Editorial Board of the international journals Sensor Review and Journal of Materials Science: Materials in Electronics. Professor White is also a Series Editor for the Integrated Microsystems series for Artech House.